RNA (2002), *8*:252–260. Cambridge University Press. Printed in the USA.

DOI: 10.1017.S1355838201014820

METHOD

Water counting: Quantitating the hydration level of paramagnetic metal ions bound to nucleotides and nucleic acids

CHARLES G. HOOGSTRATEN and R. DAVID BRITT
Department of Chemistry, University of California at Davis, Davis, California 95616, USA

ABSTRACT

Binding of divalent metal ions plays a key role in the structure and function of ribozymes and other RNAs. In turn, the energetics and kinetics of the specific binding process are dominated by the balance between the cost of dehydrating the aqueous ion and the energy gained from inner-sphere interactions with the macromolecule. In this work, we introduce the use of the pulsed EPR technique of ^{2}H Electron Spin-Echo Envelope Modulation (ESEEM) to determine the hydration level of Mn^{2+} ions bound to nucleotides and nucleic acids. Mn^{2+} is an excellent structural and functional mimic for Mg^{2+}, the most common divalent ion of physiological interest. Comparison of data in D_2O and H_2O, with aqueous Mn^{2+} as a reference standard, allows a robust and precise determination of the number of bound water molecules, and therefore the number of RNA-derived ligands. Examples of applications to the mononucleotide models MnGMP and MnATP, as well as to the paradigmatic RNA system $tRNA^{Phe}$, are shown.

Keywords: ATP, EPR, ESEEM, GMP, manganese, tRNA

INTRODUCTION

The structure and function of nucleic acids are dependent on the identity and manner of binding of associated cations. In particular, most catalytic RNA systems use specifically bound divalent metal ions both to stabilize three-dimensional structure and to participate directly in catalysis (Pyle, 1993; Feig & Uhlenbeck, 1999). The thermodynamics of specific cation–RNA association are dominated by the balance between the free energy required to partially dehydrate the aqueous ion and that gained from ligation to functional groups on the RNA (Draper & Misra, 1998; Misra & Draper, 1998, 2001). Therefore, the extent of dehydration of divalent cations bound to RNA is a key parameter in the energetics of the binding process, as well as a central consideration in the structural effects and catalytic roles of bound ions. This parameter, however, has proven difficult to measure directly in solution. The luminescence of lanthanide ions such as Eu^{3+} and Tb^{3+} (Horrocks & Sudnick, 1979, 1981) has been used for hydration analysis in systems including tRNA (Draper, 1985) and the hammerhead ribozyme (Feig et al., 1999). Such ions, however, are relatively poor mimics for the presumed physiologically relevant species Mg^{2+}. Indeed, Tb^{3+} is an inhibitor of the hammerhead ribozyme (Feig et al., 1998), and lanthanides are not known to support catalysis in any ribozyme system. In contrast, the paramagnetic metal ion Mn^{2+} is capable of replacing Mg^{2+} in most ribozymes, including the large and complex group I ribozyme and RNase P (Pyle, 1993). Mn^{2+} is an excellent structural mimic for Mg^{2+} on fundamental considerations of inorganic chemistry as well, although the increased preference of Mn^{2+} for nitrogen and sulfur ligands may lead to changes in site structure in some cases (Bock et al., 1999).

In principle, Mn^{2+} EPR spectra contain sufficient information to determine hydration levels based on line splittings arising from hyperfine couplings to solvent nuclei (^{1}H, ^{2}H, or ^{17}O; Reed & Markham, 1984). Inhomogeneous broadening of Mn^{2+} EPR signals, however, renders such splittings undetectable in conventional continuous-wave EPR spectra (but see Reed & Poyner, 2000, and references therein). Pulsed EPR techniques, in contrast, can overcome the effects of inhomogeneous broadening via the formation of spin echoes (Britt, 1995; Prisner et al., 2001). In the electron spin-echo envelope modulation (ESEEM) experiment, an electron spin echo is formed by a series of two or three high-power

Reprint requests to: R. David Britt, Department of Chemistry, University of California at Davis, One Shields Avenue, Davis, California 95616, USA; e-mail: rdbritt@ucdavis.edu

microwave pulses, and the amplitude of the echo is monitored as the interpulse delay is increased. The echo intensity is modulated by oscillations observed at frequencies characteristic of magnetic nuclei coupled to the unpaired electron spin (Mims & Peisach, 1981). Because the modulation depth increases with the number of coupled nuclei in a well-understood manner (Kevan, 1979), the number of water molecules bound to a paramagnetic ion can be determined from ^{2}H ESEEM spectra recorded in D_2O solvent. If the Mn^{2+} ion is assumed to be six-coordinate octahedral, the number of macromolecular ligands that have displaced inner-sphere aqua ligands in the bound complex is then simply the difference between six and the measured hydration number. This technique was first used by Peisach and coworkers to distinguish Mn^{2+} monohydrate from dihydrate when bound to Staphylococcal nuclease (Serpersu et al., 1988). In this report, we demonstrate appropriate methodologies for the use of ^{2}H ESEEM to determine reliably and precisely the hydration level of Mn^{2+} ions bound to nucleotides and nucleic acids, for which highly hydrated metal ions will be common. In an earlier publication (Hoogstraten et al., 2002), we showed preliminary results in a mononucleotide system; here, we present full details of the method's capabilities and pitfalls, and we demonstrate its applicability to macromolecular systems using yeast $tRNA^{Phe}$.

RESULTS

Data treatment

For the determination of hydration level, we perform three-pulse (stimulated-echo) ESEEM spectroscopy under conditions such that signals arising from ^{1}H are not observed (see Materials and Methods). Modulations in time-domain ESEEM spectra taken in D_2O solvent thus arise from three sources: (1) magnetic nuclei on the macromolecule, largely ^{14}N and ^{31}P in the absence of isotopic labeling; (2) outer-sphere and distant solvent ^{2}H nuclei; (3) ^{2}H nuclei on inner-sphere waters of hydration, the signals of interest for the present purpose (Fig. 1). Mathematically, the experimental modulation function is the product of the various contributions; therefore, the contribution of interest may be isolated by taking the quotient of the experimental data with data obtained on control samples containing the undesired, interfering contribution(s) (Mims et al., 1990). As discussed in more detail in Materials and Methods, we use a total of four samples for this purpose: Mn^{2+} complexes with the nucleic acid of interest in both D_2O and H_2O solvent, and Mn^{2+} complexes with diethylenetriaminepentaacetic acid (DTPA), a chelating agent that leaves no inner-sphere sites occupied with aqua ligands (Hoard & Stezowski, 1984; Serpersu et al., 1988), again in both D_2O and H_2O solvent (Fig. 1).

The isolation of ^{2}H ESEEM arising from inner-sphere solvent ligands is illustrated in Figure 2A, which shows raw ESEEM data in H_2O and D_2O for hexaquo Mn^{2+}, along with the D_2O/H_2O ratio. Couplings to solvent ^{2}H give rise to strong modulations with an approximate period of 500 ns, corresponding to the ^{2}H nuclear frequency at this magnetic field. Data for the outer-sphere-only MnDTPA complex is shown in Figure 2B, and Figure 2C shows the final processed modulation curve, representing pure inner-sphere ^{2}H ESEEM in hexaquo Mn^{2+}. We note that, although all samples in D_2O show modulations at the ^{2}H resonance frequency, the inner-sphere modulations in Figure 2C damp out much more rapidly than the outer-sphere modulations in MnDTPA, in accordance with expectations based on the greater anisotropy of short-range hyperfine couplings (Kevan, 1979). The rapid damping of final data thus provides a valuable check on the success of the DTPA-ratio procedure for removing outer-sphere contributions. An approximate quantitation of the effect of distance on damping is obtained by observing the time at which the echo modulation nulls and reappears with reversed phase (Kevan, 1979; arrow in Fig. 2C), which in this case (and neglecting the effects of isotropic hyperfine components), leads to an estimate of 3.0 Å for the Mn-^{2}H distance, in good accord with the value of 2.8–2.9 Å observed using ^{1}H ENDOR of Mn^{2+} in frozen aqueous solution (Tan et al., 1993). The observation of this phase reversal at the appropriate delay provides strong evidence that inner-sphere ^{2}H contributions dominate the final processed data.

Mononucleotide test cases: MnGMP and MnATP

In a comprehensive structural investigation of the MnGMP complex using ESEEM and electron spin-echo electron-nuclear double resonance (ESE-ENDOR), we found the Mn^{2+} ion to take a single inner-sphere ligand (N7) from the nucleotide, implying a pentahydrate structure (Hoogstraten et al., 2002). This same configuration was found for MnGMP in the crystal state (de Meester et al., 1974). MnGMP was therefore used as a first test case for the water-counting methodology.

Figure 3 shows experimental three-pulse ESEEM data for Mn^{2+} ligated to GMP, treated to isolate contributions from inner-sphere D_2O, at three different magnetic fields corresponding to maxima in the field-swept ESE-EPR spectrum (Fig. 3D). Expected curves for the cases of one to six inner-sphere waters of hydration, derived from experimental data for the $Mn(H_2O)_6$ complex, are shown for comparison. At each field, the data are visually consistent with a pentahydrate structure, judged primarily by the initial depth of ^{2}H modulation. Quantitative analysis of the data (Materials and Methods) yields a hydration level of 5.2 ± 0.1. These results are fully consistent with our earlier analysis indicating a

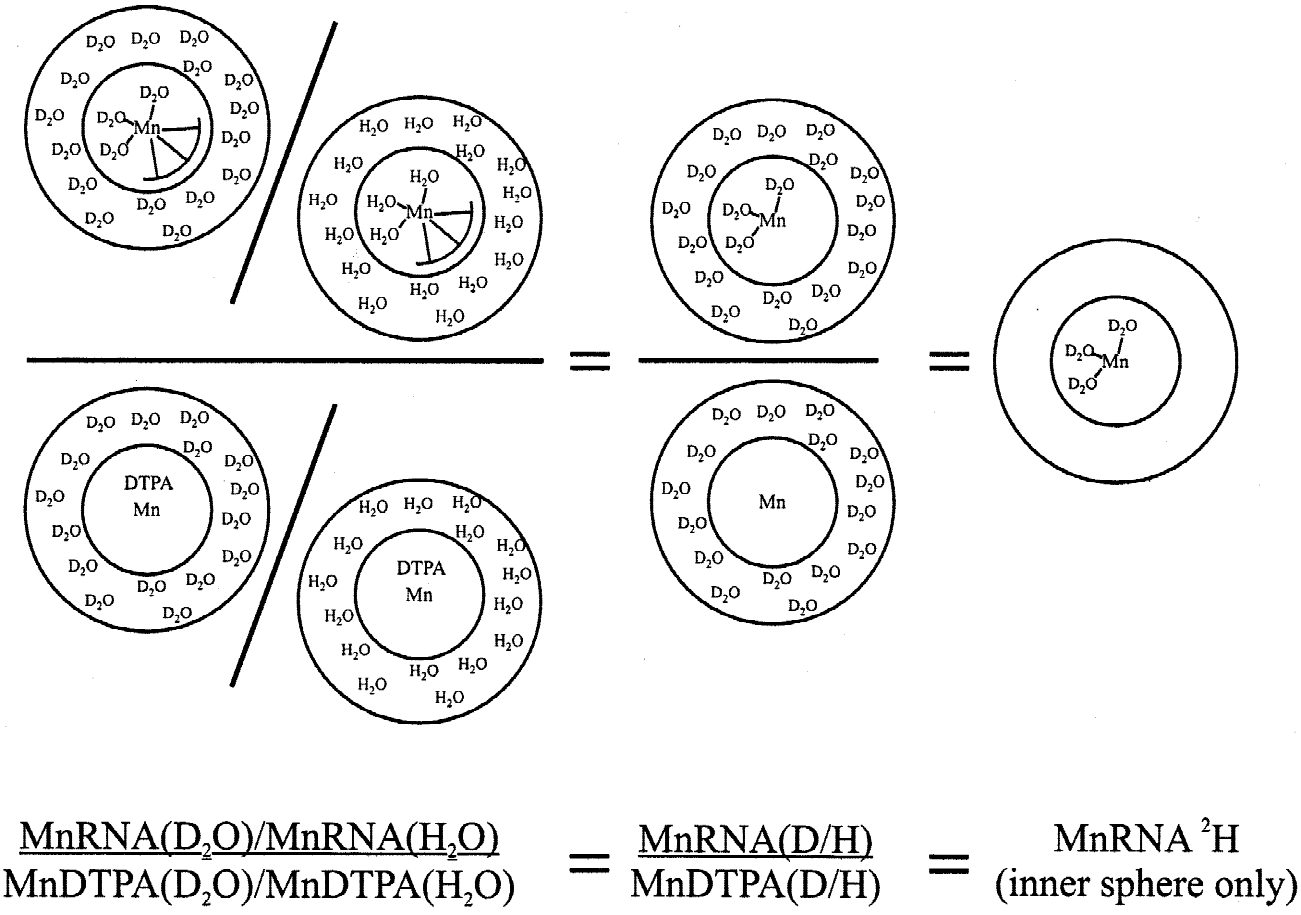

FIGURE 1. Schematic of ESEEM data treatment. Illustration of the isolation of spectral contributions of inner-sphere D_2O molecules using a ratio of ratios for four different samples (see text). The unknown sample ("MnRNA") is drawn with three solvent and three RNA-derived ligands. The ratio of identical samples in D_2O and H_2O serves to remove contributions from the macromolecule or DTPA chelate (first equality), and the ratio of data for the unknown sample to MnDTPA removes contributions from second-shell and distant solvent, leaving pure inner-sphere ^2H ESEEM (second equality). The left-hand side thus corresponds to the expression in equation (1) (Materials and Methods). Note that ESEEM contributions from ^1H nuclei, in solvent or elsewhere, are removed by the choice of experimental parameters.

single nucleotide-derived ligand to the octahedral Mn^{2+} (Hoogstraten et al., 2002).

Because of the biological importance of ATP and the common use of Mn^{2+} complexes of adenine nucleotides as spectroscopic probes of enzyme active sites, the complex of Mn^{2+} with ATP has been thoroughly investigated by a number of methods (Aoki, 1996; Sigel & Song, 1996; and references therein). Sigel and coworkers determined that ligation of Mn(II) to the triphosphate moiety of MnATP is extended into a macrochelate structure by additional ligation to the heterocyclic nitrogen N7 to an extent of 17% ± 10%, but they could not distinguish between inner- and outer-sphere ligation to N7 (Sigel 1987; Sigel et al., 1987). Using ultraviolet probes of the aromatic ring, Mariam and Martin (1979) estimated an occurrence of 10% for the N7 inner-sphere complex but stated that this analysis was not highly quantitative. In addition, even for this well-characterized complex, the number of inner-sphere ligands derived from ATP phosphates, and therefore the hydration level of the Mn^{2+} ion, has not been determined with precision. ESEEM of solvent-derived ^2H provides direct structural data that bear on these questions. For a sample containing equimolar Mn^{2+} and ATP, we find (Fig. 4) a hydration level of 3.8 ± 0.1, from which we conclude that Mn^{2+} in 1:1 complex with ATP exists on average as a tetrahydrate. Using ^{14}N ESEEM, we found no evidence for direct ligation to nitrogen in a 1:1 MnATP complex (C.G. Hoogstraten, C.V. Grant, and R.D. Britt, in prep.), implying that all non-aqua ligands derive from phosphate groups. Our data do not exclude a fraction of the complex existing as an outer-sphere macrochelate to N7, but any inner-sphere macrochelate is present at a level too low to be detectable using ESEEM.

Our results lead to the model shown in Figure 5 for the complex structure. We note that the illustrated bi-phosphate (tetrahydrate) coordination at Mn^{2+} is an ensemble average. For example, equal quantities of monophosphate- and triphosphate-coordinated Mn^{2+}

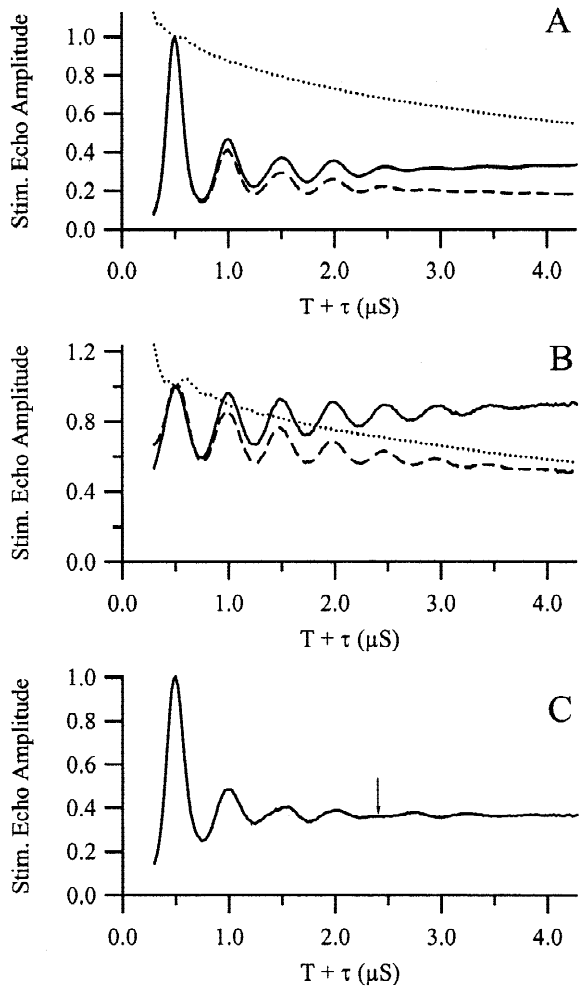

FIGURE 2. Example of data processing. Three-pulse ESEEM time-domain data and corresponding ratios for $Mn(H_2O)_6$. **A**: Raw data for $MnCl_2$ dissolved in D_2O (dashed line), H_2O (dotted line), and D/H ratio (solid line). **B**: Corresponding curves for MnDTPA. **C**: Curve describing the isolated inner-sphere ^2H interactions, obtained as the ratio of the solid curves in **A** and **B**. The arrow indicates the approximate location of a reversal of phase in the modulation, from which an apparent Mn-^2H distance was calculated (see text).

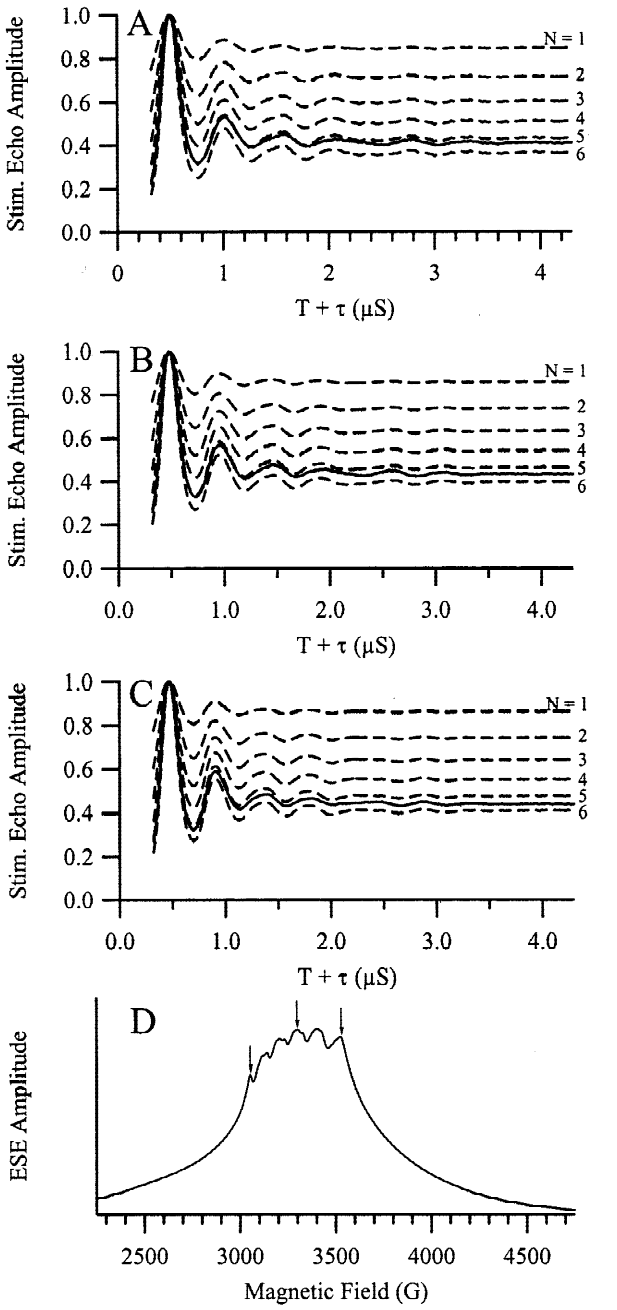

FIGURE 3. Hydration analysis for MnGMP. Determination of the number of bound water molecules in the 1:1 MnGMP complex. The solid line is experimental data for the complex, and the dashed lines are the expected data for various levels of hydration (calculated from data for $Mn(H_2O)_6$). **A**, **B**, and **C** show data collected at the field positions indicated on the Mn(II) ESE-EPR lineshape shown in **D**.

(penta- and trihydrate, respectively) would provide indistinguishable experimental data from a homogeneous biphosphate population. Within the biphosphate case, the present data also do not distinguish between $\beta - \gamma$ ligation, as drawn, and the alternate $\alpha - \beta$ and $\alpha - \gamma$ cases. Both types of heterogeneity, as well as further stereoisomerism not considered here, are well known to occur in divalent metal complexes with nucleoside triphosphates (reviewed in Saenger, 1984; Klevickis & Grisham, 1996). Nevertheless, the present estimate of the average hydration level should be useful in interpreting chemical and enzymological data. Indeed, the results shown here have aided us in deconvoluting data obtained on higher-order complexes of Mn^{2+} observed in excess ATP (C.G. Hoogstraten, C.V. Grant, and R.D. Britt, in prep.). For both mononucleotide cases, the ^2H ESEEM method has provided data of sufficient precision to quantify the hydration level to within a single aqua ligand per Mn^{2+}, and results consistent with other chemical and spectroscopic data have been obtained.

Application to a structured RNA: Yeast $tRNA^{Phe}$

Phenylalanine tRNA from the yeast *Saccharomyces cerevisiae* has long been a paradigm for studies of

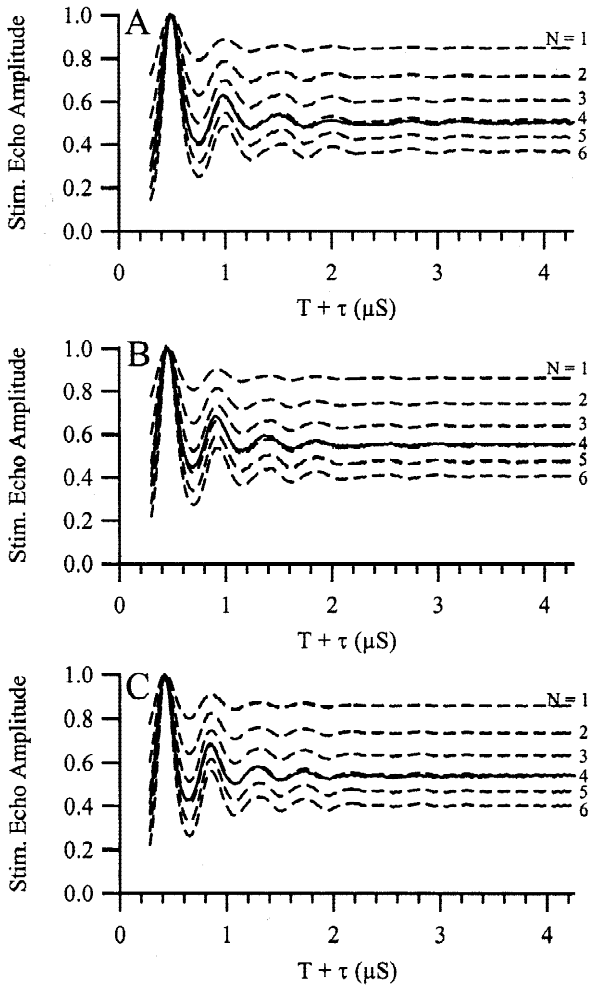

FIGURE 4. Hydration analysis for MnATP. Determination of the number of bound water molecules for a 1:1 complex of Mn^{2+} with ATP. Conventions as in Figure 3.

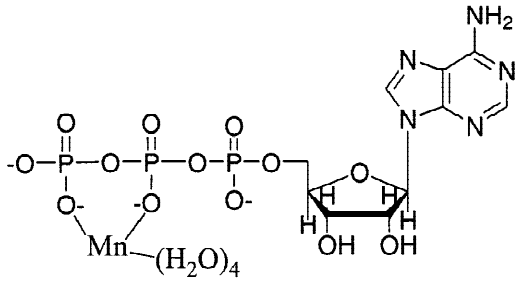

FIGURE 5. Structural model for MnATP. Configuration of the 1:1 MnATP complex based in part on the data in Figure 4.

structure, biophysics, and cation interactions in RNA (reviewed in Schimmel & Redfield, 1980). At low ionic strength, tRNA molecules bind between three and six divalent ions in a cooperative fashion (Schimmel & Redfield, 1980; Feig & Uhlenbeck, 1999). This cooperativity, however, arises from coupling to the formation of tRNA tertiary structure. At higher monovalent salt concentrations, where the tertiary structure forms in the absence of divalent ions, no cooperative binding is observed, and the number of strongly or uniquely bound divalent ions decreases significantly (Stein & Crothers, 1976; Leroy & Guéron, 1977; Walters et al., 1977; Misra & Draper, 2000). At 200 mM NaCl, for example, $tRNA^{Phe}$ binds one or at most two Mn^{2+} ions with high affinity (Leroy & Guéron, 1977). When the molecule was crystallized in the presence of Mg^{2+} and the resulting crystals were soaked in Mn^{2+}, a single high-occupancy site with five aqua ligands and one RNA-derived ligand (the N7 of G20) was found (Jack et al., 1977). A recent structural refinement using the same crystal form, however, revised the ligand assignments to this ion somewhat, and an additional two sites were found to be fully or partially occupied with Mn^{2+} (Shi & Moore, 2000), emphasizing the difficulty of drawing comparisons between ionic conditions in the crystalline and solution states. Here, we used the binding of Mn^{2+} with $tRNA^{Phe}$ to test the applicability of the ^2H ESEEM method to paramagnetic metal ion complexes with large, structured RNA molecules.

ESEEM results for a 1:1 complex of Mn to $tRNA^{Phe}$ are shown in Figure 6. As for MnGMP, the data are consistent with pentahydrate Mn^{2+} (number of aqua ligands 5.2 $\pm$ 0.2). In a similarly prepared sample, we identified a single RNA-derived Mn^{2+} ligand as a base ring nitrogen using ^{14}N ESEEM (Hoogstraten et al., 2002), in agreement with the pentahydrate structure found here. For a macromolecule such as $tRNA^{Phe}$, additional data is necessary to specify the location of the partially dehydrated ion within the structure. In some cases, specific isotope labeling in combination with ESEEM or ENDOR spectroscopy may be of assistance (e.g., Morrissey et al., 1999, 2000). Paramagnetic broadening of lines in solution-state NMR, however, provides the most general method for site identification (Feigon et al., 2001; Gonzalez & Tinoco, 2001). Hurd et al. (1979) performed such studies on three class 1 tRNA species, closely related to but not including the $tRNA^{Phe}$ used here, in both excess Mg^{2+} and high-salt, Mg^{2+}-free conditions. These authors concluded that the initial tight-binding site was near the phosphate of U8, in the region of one of the metal sites identified by Shi and Moore (2000) as partially filled with Mn^{2+}. It should be noted that crystallographic mother liquors for tRNA normally include polycations such as spermine, potentially perturbing the binding sites of divalent cations. Although sites in the elbow region of the tRNA structure, where the folded tRNA structure forms pockets of strong electrostatic potential, are plausible candidates for the tight binding site at 200 mM salt that we are analyzing here, further data is therefore necessary to identify the exact site of ion ligation within the $tRNA^{Phe}$ structure.

In contrast to the situation in high-resolution NMR, no degradation in spectral quality is seen between a monomer and a large structured RNA in ESEEM, as the experiments are performed in frozen solution where

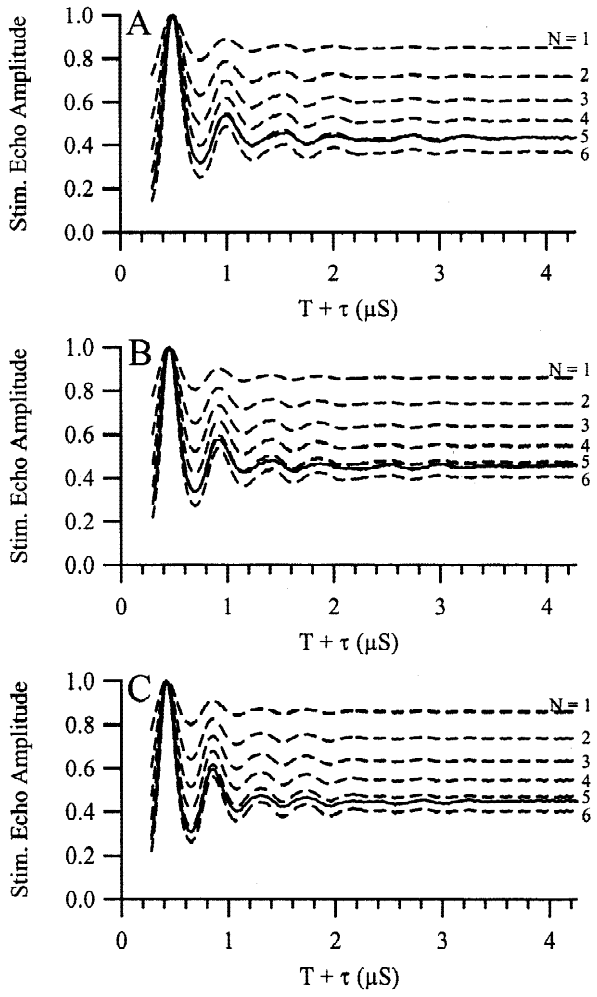

FIGURE 6. Hydration analysis for MntRNA. Determination of the number of bound water molecules for Mn^{2+} bound to yeast $tRNA^{Phe}$ in 200 mM NaCl. Conventions as in Figure 3.

the effects of molecular hydrodynamics are negligible. The experimental signal-to-noise ratio is limited by the solubility of the compound under study, but this condition has not been a limitation in the systems examined thus far due to the intrinsically high sensitivity of ^2H ESEEM. The main challenge for a particular macromolecular application is therefore likely to be the requirement for isolation of a single bound paramagnetic ion (see Discussion). Given these conditions, however, the results for tRNA shown here demonstrate that ^2H ESEEM gives precise and robust results for Mn^{2+} hydration whether the ligand is a mononucleotide or a much larger system.

Choice of cryoprotectant

Because Mn^{2+} ESEEM is performed at cryogenic temperatures (4.2 K, in this work), a glassing agent or cryoprotectant must be added to the liquid sample before freezing to prevent solute segregation and other adverse effects. Many common cryoprotectants, however, contain hydroxylic functional groups, which can themselves occupy coordination sites on metal ions. Errors due to an inappropriate choice of cryoprotectant must thus be considered. For example, Halkides et al. (1998) demonstrated that glycerol, a commonly used and very effective cryoprotectant, ligates directly to Mn^{2+} bound in the active site of p21-*ras* by displacing aqua ligands.

To address the issue of the proper cryoprotectant for use in the experiments described here, we compared ^2H ESEEM data for $Mn(H_2O)_6$ cryoprotected in three different ways. (Attempts to acquire data in a carefully frozen but noncryoprotected sample failed due to the inability to detect a reproducible spin-echo.) The effectiveness of cryoprotection was judged by the rate of echo decay in two-pulse ESEEM, the so-called "phase memory time." We observed the most effective cryoprotection in 50% glycerol, followed by 20% ethylene glycol, with 0.4 M sucrose performing significantly worse than either (data not shown), in agreement with observations by others (Halkides et al., 1998). Figure 7A shows three-pulse ESEEM D_2O/H_2O ratios for these three samples, and demonstrates a substantial decrease in solvent-derived ^2H ESEEM modulation for $Mn(H_2O)_6$ in glycerol, consistent with the occupation of inner-sphere coordination sites by the cryoprotectant

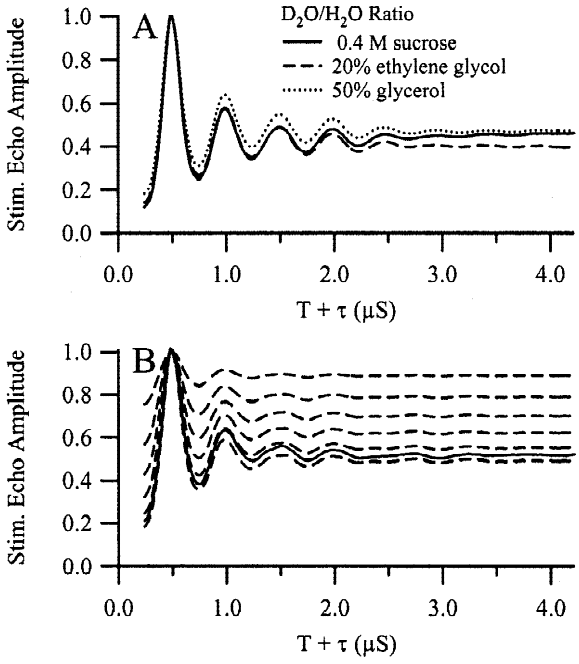

FIGURE 7. Effect of varying cryoprotectant on ESEEM data. **A**: Ratio of three-pulse ESEEM data collected in D_2O to H_2O for $Mn(H_2O)_6$ in the indicated cryoprotection conditions. **B**: Apparent hydration level of an ethylene glycol-protected sample (solid line) assessed using reference curves constructed via $Mn(H_2O)_6$ cryoprotected in sucrose (dashed lines). Overall modulation is shallower than in Figures 3, 4, and 6 due to use of a shorter spin-echo delay τ for these experiments.

in this case. The curves for ethylene glycol and sucrose, by contrast, are very similar. For quantitative analysis of the latter two curves, we acquired comparable data for a complex of MnDTPA cryoprotected with either 20% ethylene glycol or 0.4 M sucrose, and used these data according to equation (1) (see below) to derive pure inner-sphere ^{2}H ESEEM for $Mn(H_2O)_6$ in ethylene glycol or sucrose. The resulting curves are shown in Figure 7B, and are consistent with ethylene glycol occupying an additional fraction of a coordination site on average relative to sucrose.

The above analysis indicates that 50% glycerol and, to a lesser extent, 20% ethylene glycol, will occupy some inner-sphere coordination sites on Mn^{2+} in aqueous solution. Because we were unable to obtain ESEEM in the complete absence of cyroprotectant, we cannot demonstrate rigorously that sucrose itself does not partially displace waters of hydration on Mn^{2+}, potentially distorting the results of water-counting ESEEM experiments. We consider this relatively unlikely, however, because the constrained ring structure of sucrose precludes the chelated structure that favors binding for unconstrained polyalcohols such as glycerol. In agreement with this contention, Halkides et al. (1998) found no evidence of the binding of deuterated methyl-α-D-glucopyranoside to Mn^{2+} using ^{2}H ESEEM. Although some possibility of error remains, therefore, we consider 0.4 M sucrose or similar saccharide-based cryoprotectants a relatively safe choice for cryoprotection in water-counting experiments, especially given the chemically and biologically reasonable results for MnGMP, MnATP, and Mn-tRNA obtained in the present study. In contrast, the use of unconstrained polyalcohols such as glycerol and ethylene glycol carries substantial risk of causing errors and should be avoided for such experiments, despite the superiority of these species as glassing agents.

DISCUSSION

Standards and calibration

For a single unpaired electron (electron spin $S = 1/2$), the number of coupled magnetic nuclei can be determined directly by numerical simulation of the ESEEM modulation pattern (Kevan, 1979; Mims & Peisach, 1981). Unfortunately, the probe ion Mn^{2+} has five unpaired valence electrons ($S = 5/2$), and exact simulations are much more difficult for this case. Therefore, the magnitude of ^{2}H echo modulations must be analyzed by reference to a convenient standard. Serpersu et al. (1988) used the single-hydrate complex MnEDTA to analyze Mn^{2+} bound to Staphylococcal nuclease, successfully distinguishing a single bound D_2O (pattern identical to the MnEDTA/MnDTPA ratio) from two bound D_2O (pattern the square of that seen in MnEDTA/MnDTPA). The uncertainties inherent in extrapolating modulation due to a single D_2O to the highly hydrated ions common in nucleotides and nucleic acids, as well as differences in the magnetic properties (particularly the zero-field splitting) of Mn^{2+} bound to a strong chelator as compared to an RNA site, render this procedure impractical for the present purposes. Indeed, our initial attempts to apply directly the technique of Serpersu et al. to nucleic acids yielded poorly reproducible and physically unrealistic results (not shown). Therefore, we used a ratio of hexaquo Mn^{2+} to MnDTPA (see Fig. 2) as a reference standard. Ions with N bound waters of hydration will show inner-sphere ^{2}H ESEEM modulation equal to the (N/6)th power of that in the standard. (We note that, due to the finite ionization of Mn^{2+}-bound H_2O, the average number of ^{2}H atoms in the first coordination sphere will be somewhat less than 12, depending on pH. As long as the pKa of Mn^{2+} bound in the site of interest is not significantly different from that in $Mn(H_2O)_6$, however, the calculation of the number of D_2O ligands in the unknown sample will be unaffected.) Using hexaquo Mn^{2+} as a standard allows one to distinguish among sites with four, five, and six waters of hydration, and therefore provides a valuable complement to MnEDTA standardization. For ions with intermediate hydration numbers, neither MnEDTA nor $Mn(H_2O)_6$ may provide a fully satisfactory reference for absolute determinations, and other types of small-molecule chelators may prove useful.[1] As an alternative, high-frequency EPR lineshape analysis for samples in $H_2{}^{17}O$, which has proven effective in the regime of $N = 2$ to $N = 4$, can be applied (Latwesen et al., 1992; Bellew et al., 1996; Bernat et al., 1997). In nucleic acid sites, however, high levels of hydration will be the norm (Draper & Misra, 1998; Feig & Uhlenbeck, 1999; Misra & Draper, 2001), and the procedures described in this article will be an appropriate choice.

For macromolecular applications of ^{2}H ESEEM, it is crucial to isolate the binding of a single paramagnetic ion, because the results obtained will be an average of all Mn^{2+} ions in the sample. The deconvolution of ESEEM data for multiple bound equivalents of Mn^{2+}, although in principle possible, will in practice be quite difficult. The availability of solution binding curves, such as those derived for $tRNA^{Phe}$ at high salt by Leroy and Guéron (1977), is thus an essential prerequisite for the design of ESEEM experiments. In the present case, the choice of 200-mM monovalent salt buffer for our tRNA sample was dictated by the requirement for conditions under which a single, unique, strongly bound ion is present.

[1]We also note that the removal of outer-sphere contributions using MnDTPA samples is not fully rigorous, due to differences in outer-sphere geometry and zero-field splitting between Mn^{2+} bound to DTPA and to macromolecules. The observation of a modulation null at the appropriate delay (e.g., Fig. 2C), however, provides a valuable check on the operational validity of this procedure for a particular sample.

SUMMARY AND PERSPECTIVE

In this work, we have demonstrated a robust spectroscopic procedure to determine the hydration level of paramagnetic divalent cations such as Mn^{2+} bound to nucleotides and nucleic acids. As demonstrated by data on mononucleotide systems as well as budding yeast $tRNA^{Phe}$, the precision of the analysis is easily good enough to detect the gain or loss of individual waters of hydration. In many situations, the precise number of waters of hydration is of key interest in sorting out the structural, energetic, and mechanistic features of metal ions that are critical to the function of ribozymes and other nucleic acids.

The determination of hydration level using ^2H ESEEM is directly complementary to a number of other EPR spectroscopic methods for investigating the ligation structure of metal ions bound to nucleotides and nucleic acids. In the case of the vanadyl ion (VO^{2+}), Makinen and coworkers have used continuous-wave electron-nuclear double resonance (CW-ENDOR) to investigate the structure of ^1H and ^{31}P ligands (Mustafi et al., 1992; Jiang & Makinen, 1995). CW-ENDOR has been applied by DeRose and coworkers to Mn^{2+} ions bound to systems including the hammerhead ribozyme (Morrissey et al., 2000). In collaboration with the DeRose group, we have analyzed heterocyclic base nitrogen ligation to Mn^{2+} using ^{14}N ESEEM (Morrissey et al., 1999). Because ENDOR is not a quantitative technique in terms of ligand number, however, and some nucleotide-derived ligand types are ESEEM silent (e.g., carbonyl groups in the absence of ^{13}C labeling), none of these studies could rigorously determine the number of aqua ligands to the metal ion in question. The ^2H ESEEM methods described here, therefore, are a valuable complement to ESEEM and CW and pulsed ENDOR analyses of nucleotide-derived ligands.

MATERIALS AND METHODS

All buffers, reagents, and nucleotides were purchased from Sigma at the highest purity available and were used without further purification, except as noted. Guanosine 5′-monophosphate and adenosine 5′-triphosphate samples were 5 mM nucleotide, 1.0 mM $MnCl_2$ and 1.2 mM nucleotide, 1.0 mM $MnCl_2$, respectively. For mononucleotide samples, the only monovalent salt was that provided by the buffer, 10 mM sodium cacodylate at pH 7.0. The yeast $tRNA^{Phe}$ sample was 0.5 mM in tRNA, 0.2 mM $MnCl_2$, 200 mM NaCl, 10 mM sodium cacodylate buffer, pH 7.0. All samples were prepared as identical pairs containing all components except cryoprotectant, lyophilized to dryness, resuspended in either H_2O or D_2O, and relyophilized several times. Cryoprotectant was added upon final resuspension and dilution. Sample volume was 120 μL. Except as noted, all samples were cryoprotected with 0.4 M sucrose (previously prepared in H_2O or D_2O as appropriate) prior to freezing and storage in liquid nitrogen.

Pulsed EPR spectroscopy was performed on a laboratory-built 8–18 GHz spectrometer previously described (Sturgeon & Britt, 1992; Sturgeon et al., 1994). Three-pulse ESEEM experiments were performed using standard methods (Kevan, 1979; Mims & Peisach, 1981). Fixed spin-echo delays τ were set to an integer multiple (usually 2 or 3; approximately 200 ns for the magnetic field values used here) of the ^1H precession period to remove modulation arising from ^1H nuclei (Mims & Peisach, 1981). All spectroscopy was performed at 4.2 K and 9.3 GHz. ESEEM experiments were repeated with the magnetic field set to three different maxima of the Mn^{2+} ESE-EPR lineshape, typically 3090, 3340, and 3570 G (Fig. 3D).

ESEEM data were normalized by setting the value at the first maximum of the ^2H modulation to unit intensity. Reported data were constructed using traces from four samples, Mn^{2+} bound to the test molecule in H_2O and D_2O and MnDTPA in H_2O and D_2O, combined according to

$$\frac{\mathrm{MnRNA}(D_2O)/\mathrm{MnRNA}(H_2O)}{\mathrm{MnDTPA}(D_2O)/\mathrm{MnDTPA}(H_2O)} \quad (1)$$

where MnRNA refers to the unknown sample or hexaquo standard, to isolate modulations due to inner-sphere D_2O ligands (Fig. 1). For some samples, variations in overall echo decay rates led to ratioed data containing a slight overall upward or downward slope. In these cases, the final data were multiplied by a weak decaying or rising exponential function to obtain a horizontal trace at long time values, as predicted by theory (Kevan, 1979), and renormalized. Standard curves for number of aqua ligands $N = 6$ were obtained by considering $Mn(H_2O)_6$ as the test sample and treating the data as usual. The $N = 6$ trace was numerically raised to the power of (N/6) to generate standard curves for lower N. For quantitative analysis, the exponent that raised the experimental curve to the closest match with the $N = 6$ curve, as judged by agreement of the depth of the first several ^2H modulations, was determined. Data from analyses performed on the same samples at three different magnetic fields was used to calculate the reported mean and standard error.

ACKNOWLEDGMENTS

This work was supported by National Institutes of Health grant GM61211 to R.D.B. The authors are grateful to Jeffrey M. Peloquin and Christopher V. Grant for helpful discussions, and to Scott K. Silverman for discussions and a careful review of the manuscript.

Received September 6, 2001; returned for revision September 26, 2001; revised manuscript received November 26, 2001

REFERENCES

Aoki K. 1996. General conclusions from solid state studies of nucleotide-metal ion complexes. In: Sigel A, Sigel H, eds. *Metal ions in biological systems, vol. 32: Interactions of metal ions with nucleotides, nucleic acids, and their constituents*. New York: Marcel Dekker. pp 91–134.

Bellew BF, Halkides CJ, Gerfen GJ, Griffin RG, Singel DJ. 1996. High frequency (139.5 GHz) electron paramagnetic resonance char-

acterization of Mn(II)-$H_2{}^{17}O$ interactions in GDP and GTP forms of p21 *ras*. *Biochemistry 35*:12186–12193.
Bernat BA, Laughlin LT, Armstrong RN. 1997. Fosfomycin resistance protein (FosA) is a manganese metalloglutatione transferase related to glyoxalase I and the extradiol dioxygenases. *Biochemistry 36*:3050–3055.
Bock CW, Katz AK, Markham GD, Glusker JP. 1999. Manganese as a replacement for magnesium and zinc: Functional comparison of the divalent ions. *J Am Chem Soc 121*:7360–7372.
Britt RD. 1995. Time-domain electron paramagnetic resonance spectroscopy. *Curr Op Struct Biol 3*:774–779.
de Meester P, Goodgame DML, Jones TJ, Skapski AC. 1974. X-ray evidence for metal-N-7 bonding in a hydrated manganese derivative of guanosine 5′-monophosphate. *Biochem J (London) 139*:791–792.
Draper DE. 1985. On the coordination properties of Eu^{3+} bound to RNA. *Biophys Chem 21*:91–101.
Draper DE, Misra VK. 1998. RNA shows its metal. *Nature Struct Biol 5*:927–930.
Feig AL, Panek M, Horrocks WD Jr, Uhlenbeck OC 1999. Probing the binding of Tb(III) and Eu(III) to the hammerhead ribozyme using luminescence spectroscopy. *Chem Biol 6*:801–810.
Feig AL, Scott WG, Uhlenbeck, OC. 1998. Inhibition of the hammerhead ribozyme cleavage reaction by site-specific binding of Tb(III). *Science 279*:81–84.
Feig AL, Uhlenbeck OC. 1999. The role of metal ions in RNA biochemistry. In: Gesteland RF, Cech TR, Atkins JF, eds. *The RNA World* (2nd ed.). Cold Spring Harbor, New York: Cold Spring Harbor Laboratory Press. pp 287–319.
Feigon J, Butcher SE, Finger LD, Hud NV. 2001. Solution nuclear magnetic resonance probing of cation binding sites on nucleic acids. *Methods Enzymol 338*:401–420.
Gonzalez RL Jr, Tinoco I Jr. 2001. Identification and characterization of metal ion binding sites in RNA. *Methods Enzymol 338*:421–443.
Halkides CJ, Farrar CT, Singel DJ. 1998. The effects of cryoprotection on the structure and activity of p21 *ras*: Implications for electron spin-echo envelope modulation spectroscopy. *J Magn Reson 134*:142–153.
Hoard JL, Stezowski JJ. 1984. Heavy-metal ionophores—correlations among structural parameters of complexed nonpeptide polyamino acids. *Isr J Chem 24*:323–334.
Hoogstraten CG, Grant CV, Horton TE, DeRose VJ, Britt RD. 2002. Structural analysis of metal ion ligation to nucleotides and nucleic acids using pulsed EPR spectroscopy. *J Am Chem Soc*. In press.
Horrocks WD Jr, Sudnick DR. 1979. Lanthanide ion probes of structure in biology. Laser-induced luminescence decay constants provide a direct measure of the number of metal-coordinated water molecules. *J Am Chem Soc 101*:334–340.
Horrocks WD Jr, Sudnick DR. 1981. Lanthanide ion luminescence probes of the structure of biological macromolecules. *Acc Chem Res 14*:384–392.
Hurd RE, Azhderian E, Reid BR. 1979. Paramagnetic ion effects on the nuclear magnetic resonance spectrum of transfer ribonucleic acid: Assignment of the 15-48 tertiary resonance. *Biochemistry 18*:4012–4017.
Jack A, Ladner JE, Rhodes D, Brown RS, Klug A. 1977. A crystallographic study of metal-binding to yeast phenylalanine transfer RNA. *J Mol Biol 111*:315–328.
Jiang FS, Makinen MW. 1995. NMR and ENDOR conformational studies of the vanadyl guanosine 5′-monophosphate complex in hydrogen-bonded quartet assemblies. *Inorg Chem 34*:1736–1744.
Kevan L. 1979. Modulation of electron spin-echo decay in solids. In: Kevan L, Schwartz RN, eds. *Time domain electron spin resonance.* New York: Wiley-Interscience. pp 279–341.
Klevickis C, Grisham CM. 1996. Phosphate-metal ion interactions of nucleotides and polynucleotides. In: Sigel A, Sigel H, eds. *Metal ions in biological systems, vol. 32: Interactions of metal ions with nucleotides, nucleic acids, and their constituents*. New York: Marcel Dekker. pp 1–26.
Latwesen DG, Poe M, Leigh JS, Reed GH. 1992. Electron paramagnetic resonance studies of a *ras* p21-Mn^{II}GDP complex in solution. *Biochemistry 31*:4946–4950.
Leroy JL, Guéron M. 1977. Electrostatic effects in divalent ion binding to tRNA. *Biopolymers 16*:2429–2446.
Mariam YH, Martin RB. 1979. Proximity of nucleic base and phosphate groups in metal ion complexes of adenine nucleotides. *Inorg Chim Acta 35*:23–28.
Mims WB, Peisach J. 1981. Electron spin echo spectroscopy and the study of metalloproteins. *Biol Magn Reson 3*:213–263.
Mims WB, Davis JL, Peisach J. 1990. The exchange of hydrogen ions and of water molecules near the active site of cytochrome *c*. *J Magn Reson 86*:273–292.
Misra VK, Draper DE. 1998. On the role of magnesium ions in RNA stability. *Biopolymers 48*:113–135.
Misra VK, Draper DE. 2000. Mg^{2+} binding to tRNA revisited: The nonlinear Poisson-Boltzmann model. *J Mol Biol 299*:813–825.
Misra VK, Draper DE. 2001. A thermodynamic framework for Mg^{2+} binding to RNA. *Proc Natl Acad Sci USA 98*:12456–12461.
Morrissey SR, Horton TE, DeRose VJ. 2000. Mn^{2+} sites in the hammerhead ribozyme investigated by EPR and continuous-wave Q-band ENDOR spectroscopies. *J Am Chem Soc 122*:3473–3481.
Morrissey SR, Horton TE, Grant CV, Hoogstraten CG, Britt RD, DeRose VJ. 1999. Mn^{2+}-Nitrogen interactions in RNA probed by electron spin echo envelope modulation spectroscopy: Application to the hammerhead ribozyme. *J Am Chem Soc 121*:9215–9218.
Mustafi D, Telser J, Makinen MW. 1992. Molecular geometry of vanadyl-adenine nucleotide complexes determined by EPR, ENDOR, and molecular modeling. *J Am Chem Soc 114*:6219–6226.
Prisner T, Rohrer M, MacMillan F. 2001. Pulsed EPR spectroscopy: Biological applications. *Annu Rev Phys Chem 52*:279–313.
Pyle AM. 1993. Ribozymes: A distinct class of metalloenzymes. *Science 261*:709–714.
Reed GH, Markham GD. 1984. EPR of Mn(II) complexes with enzymes and other proteins. *Biol Magn Reson 6*:73–142.
Reed GH, Poyner RR. 2000. Mn^{2+} as a probe of divalent metal ion binding and function in enzymes and other proteins. In: Sigel A, Sigel H, eds. *Metal ions in biological systems, vol. 32: Interactions of metal ions with nucleotides, nucleic acids, and their constituents*. New York: Marcel Dekker. pp 183–207.
Saenger W. 1984. *Principles of nucleic acid structure*. New York: Springer-Verlag. pp 201–219.
Schimmel PR, Redfield AG. 1980. Transfer RNA in solution: Selected topics. *Ann Rev Biophys Bioeng 9*:181–221.
Serpersu EH, McCracken J, Peisach J, Mildvan AS. 1988. Electron spin echo modulation and nuclear relaxation studies of Staphylococcal nuclease and its metal-coordinating mutants. *Biochemistry 27*:8034–8044.
Shi H, Moore PB. 2000. The crystal structure of yeast phenylalanine tRNA at 1.93 Å: A classic structure revisited. *RNA 6*:1091–1105.
Sigel H. 1987. Isomeric equilibria in complexes of adenosine 5′-triphosphate with divalent metal ions: Solution structures of $M(ATP)^2$ complexes. *Eur J Biochem 165*:65–72.
Sigel H, Song B. 1996. Solution structures of nucleotide-metal ion complexes. Isomeric equilibria. In: Sigel A, Sigel H, eds. *Metal ions in biological systems, vol. 32: Interactions of metal ions with nucleotides, nucleic acids, and their constituents*. New York: Marcel Dekker. pp 135–205.
Sigel H, Tribolet R, Malini-Balakrishnan R, Martin RB. 1987. Comparison of the stabilities of monomeric metal ion complexes formed with adenosine 5′-triphosphate (ATP) and pyrimidine-nucleoside 5′-triphosphates (CTP, UTP, TTP) and evaluation of the isomeric equilibria in the complexes of ATP and CTP. *Inorg Chem 26*: 2149–2157.
Stein A, Crothers DM. 1976. Equilibrium binding of magnesium(II) by *Escherichia coli* $tRNA^{fMet}$. *Biochemistry 15*:157–160.
Sturgeon BE, Ball JA, Randall DW, Britt RD. 1994. ^{55}Mn electron spin echo ENDOR of Mn^{2+} complexes. *J Phys Chem 98*:12871–12883.
Sturgeon BE, Britt RD. 1992. Sensitive pulsed EPR spectrometer with an 8 to 18 GHz frequency range. *Rev Sci Instrum 63*:2187–2192.
Tan X, Bernardo M, Thomann H, Scholes CP. 1993. Pulsed and continuous wave electron nuclear double resonance patterns of aquo protons coordinated in frozen solution to high spin MN^{2+}. *J Chem Phys 98*:5147–5157.
Walters JALI, Geerdes HAM, Hilbers CW. 1977. On the binding of Mg^{2+} and Mn^{2+} to tRNA. *Biophys Chem 7*:147–151.